Physics Letters B 749 (2015) 592–596

Contents lists available at ScienceDirect

Physics Letters B

www.elsevier.com/locate/physletb

Probing the quark–gluon interaction with hadrons

Hèlios Sanchis-Alepuz *, Richard Williams *

Institut für Theoretische Physik, Justus-Liebig–Universität Giessen, 35392 Giessen, Germany

ARTICLE INFO

Article history:
Received 23 June 2015
Received in revised form 31 August 2015
Accepted 31 August 2015
Available online 2 September 2015
Editor: W. Haxton

Keywords:
Quark–gluon vertex
Baryons
Mesons
QCD's Green's functions

ABSTRACT

We present a unified picture of mesons and baryons in the Dyson–Schwinger/Bethe–Salpeter approach, wherein the quark–gluon and quark–(anti)quark interactions follow from a systematic truncation of the QCD effective action and include all its tensor structures. The masses of some of the ground-state mesons and baryons are found to be in reasonable agreement with the expectations of a 'quark-core calculation', suggesting a partial insensitivity to the details of the quark–gluon interaction. However, discrepancies remain in the meson sector, and for excited baryons, that suggest higher order corrections are relevant and should be investigated following the methods outlined herein.

1. Introduction

Hadrons provide a rich experimental environment for the study of the strong interaction, from details of the resonance spectrum to form factors and transition decays via electromagnetic probes. These reflect the underlying substructure of bound states by resolving, in a non-trivial way, the quarks and gluons of which they are composed. A theoretical understanding of hadrons in terms of these underlying degrees of freedom, interacting as dictated by quantum chromodynamics (QCD), is an on-going effort. Many approaches tackle it in different ways, simplifying certain aspects of the theory. Probing sensibly our theoretical constructs with experimental input thus provides understanding of the theory itself.

In continuum approaches to QCD, it is not possible in general to include all possible correlation functions in a calculation, as there are infinitely many of them. Although this can be viewed as a limitation of continuum approaches, only a finite number of these correlation functions have a significant role in the observable properties of hadrons. Therefore, by including a greater number of relevant correlation functions into the system, continuum methods provide an ideal framework to unravel the underlying mechanisms that generate observable effects from the elementary and non-observable degrees of freedom of QCD. This is in contrast to lattice QCD calculations, which can be viewed as theoretical experiments in the sense that, although they contain *a priori* all the dynamics of QCD, it is challenging to single out individual contributions to a particular measurement. This makes these two approaches complementary.

Amongst the different continuum approaches, the combination of Dyson–Schwinger (DSE) and Bethe–Salpeter equations (BSE) has proven to be extremely useful in the calculation of hadronic properties from QCD [1–3]. Typically, solutions of DSEs constitute the building blocks (propagators and vertices) of bound-state calculations using BSEs, which provide the bridge between QCD and observables. As described in more detail below, the interaction terms that are kept in the DSE determine the interaction kernels among constituents in the BSEs, thereby defining a particular truncation of the DSE/BSE system. One works towards a model-independent truncation by including a larger set of interaction terms; although this programme is obviously not achievable in its totality, it is expected that there will be some degree of convergence at the level of this vertex expansion.

Here we focus upon the inclusion of the quark–gluon interaction, the reliable construction of which is a challenging task. However, one is guided by various symmetries – notably that of chiral symmetry – that provide for stringent constraints. To implement these symmetries at the level of the quark and gluon interaction, simplifications are clearly necessary which typically fall into three categories: (i) the quark–gluon vertex is truncated to its tree-level component times a momentum-dependent effective coupling with the quark DSE and hadron BSEs solved self-consistently [4,5]; (ii) a more sophisticated model for the quark–gluon vertex is used, with the contribution from its different tensor structures modelled,

* Corresponding authors.
E-mail addresses: helios.sanchis-alepuz@physik.uni-giessen.de (H. Sanchis-Alepuz), richard.williams@physik.uni-giessen.de (R. Williams).

http://dx.doi.org/10.1016/j.physletb.2015.08.067

hence abandoning self-consistency but gaining instead flexible insight into the relative importance of each of these structures [6–9]; (iii) some non-perturbative effects of the quark and gluon interaction are taken into account by solving the quark–gluon vertex DSE self-consistently, but potentially introducing some truncation artifacts [10–12]. We follow here the latter approach, since as we demonstrate in this letter it enables the controlled inclusion of interaction mechanisms based on a loop expansion of the effective action.

The effective action is a generating functional for proper vertex functions, and may be considered as a means to define the quantum field theory given an action, since all necessary Green's functions can be derived from it. Related are the n-particle irreducible (nPI) effective actions that form a family of different, but equivalent, representations of the same generating functional (see, *e.g.* [13]). They are defined as functionals of all $m \leq n$ Green's functions of the theory (fields, propagators, vertices, etc.). Although its exact form is not known in general, its loop expansion in $\hbar$ is well-defined [13] and can in practice be performed. Moreover, each term in the expansion already captures both perturbative and non-perturbative physics.

One reason that makes nPI techniques a powerful tool is that they provide a natural link between bound-state equations described by BSEs and the propagators and vertices provided by DSEs [14–18]. A truncation of the loop expansion at a certain order translates into a unique prescription for the truncation of the DSEs and the BSEs that maintains symmetries. For the study of two- and three-body states, it suffices to use either the 2PI effective action, which is defined in terms of fully-dressed propagators but bare vertices [19], or the 3PI effective action, which is defined also in terms of the fully-dressed vertices. In this work we restrict ourselves to the 2PI case and defer the use of the 3PI effective action to a future and more comprehensive study.

In connection with the three categories outlined above, it is worth mentioning here that the somewhat hybrid possibility of supplementing some of QCDs degrees of freedom in favor of effective ones, such as pions, has also been explored [20–25]. These can be viewed as approximate representations of the four-quark vertex in the 4PI formalism that introduces at the first step decay channels and a mixing with tetraquark states.

In the present work, we incorporate the results of a recent study of the quark–gluon vertex from a truncated DSE [12] in the calculation of meson and baryon masses. That truncation can be interpreted in the context of the 2PI effective action at 3-loop. Although on the technical side this is no novelty for meson calculations [11,26], it is the first time that corrections incorporating the gluon self-interaction have been included in the covariant three-body baryon calculation. While there exist other recent investigations of the quark–gluon vertex [27–29], these have not yet been confronted with the challenge of reproducing hadron phenomena for reasons we discuss below.

Finally, we wish to stress that this work represents only the first step in an on-going effort to incorporate realistic QCD's Green's functions into the self-consistent study of bound states. Not surprisingly, the low-order of the truncation used performs only as well as simple phenomenological models such as rainbow-ladder. However, but most importantly, it serves as a proof of principle that such an endeavor is feasible, as further increasing the order of the truncation does not increase the technical complexity dramatically.

2. Framework

The starting point for the study of hadronic observables in the present framework is thus the effective action

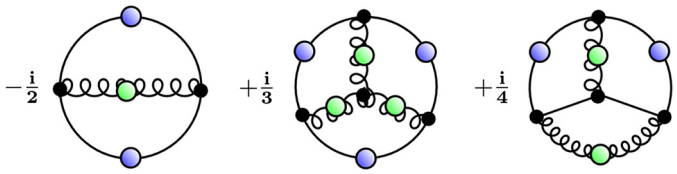

Fig. 1. The 2-particle irreducible term $\Gamma_2[\Psi, G]$ in the definition of the effective action, up to three loops.

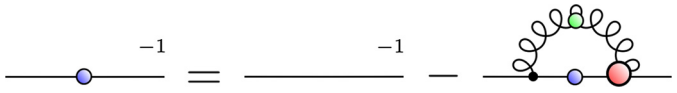

Fig. 2. The Dyson–Schwinger equation for the quark propagator.

$$\Gamma[\Psi, G] = \mathrm{S}[\Psi] + i\,\mathrm{Tr}\log G - i\,\mathrm{Tr}\,G_0^{-1}G + \Gamma_2[\Psi, G]\,, \tag{1}$$

where S is the classical action, and Ψ and G collectively represent the fields and full propagators of QCD, respectively. The term $\Gamma_2[\Psi, G]$ contains two-particle irreducible diagrams only and G_0 denotes the classical propagators. To proceed, we perform a loop expansion of $\Gamma_2[\Psi, G]$ to three-loop order, as shown in Fig. 1. Moreover, we keep only the non-Abelian term that connects the gauge to the matter sector and neglect the Abelian correction (third diagram), as it is expected to be subleading in the large-N_c limit; whether this is indeed the case for the description of hadron phenomena must certainly be tested and will be the subject of future work.

The next basic element in meson and baryon calculations is the fully-dressed quark propagator. It is given by the quark DSE, see Fig. 2

$$S^{-1}(p;\mu) = Z_2 S_0^{-1}(p) + \Sigma(p;\mu)\,, \tag{2}$$

with quark self-energy

$$\Sigma(p;\mu) = g^2 Z_{1f} C_F \int_k \gamma^\mu S(q)\Gamma^\nu(q,p) D_{\mu\nu}(k)\,. \tag{3}$$

Here $q = k + p$, the integral measure is $\int_k = \int d^4k/(2\pi)^4$ and Z_{1f}, Z_2 are renormalization constants for the quark–gluon vertex and quark propagator respectively. It is clearly dependent upon both the gluon propagator $D_{\mu\nu}(k)$ and the quark–gluon vertex $\Gamma^\nu(q,p)$. The (Landau gauge) propagators are

$$S^{-1}(p) = Z_f^{-1}(p^2)\left(i\not{p} + M(p^2)\right)\,, \tag{4}$$

$$D^{\mu\nu}(k) = T^{\mu\nu}_{(k)} Z(k^2)/k^2\,, \tag{5}$$

with quark wavefunction $Z_f^{-1}(p^2)$, dynamical mass $M(p^2)$ and gluon dressing $Z(k^2)$. The transverse projector is $T^{\mu\nu}_{(k)} = \delta^{\mu\nu} - k^\mu k^\nu/k^2$. From the 2PI effective action, the quark DSE is determined via a functional derivative with respect to the quark propagator

$$\Sigma = -i\frac{\delta\Gamma_2}{\delta G}\,. \tag{6}$$

The expansion of the effective action in Fig. 1 thus defines a truncation of the quark DSE, which is equivalent to the truncation of the quark–gluon vertex DSE shown in Fig. 3. Specifically, the truncated vertex DSE can be given as a summation of vertex corrections

$$\Gamma^\mu(l,k) = Z_{1f}\gamma^\mu + \Lambda^\mu_{\mathrm{NA}} + \ldots\,, \tag{7}$$

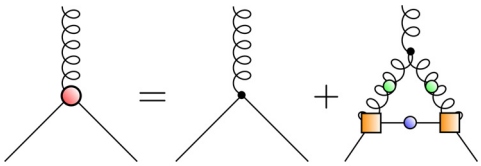

Fig. 3. The truncated DSE for the quark–gluon vertex, showing the non-Abelian correction. Boxes represent an RG improvement of the bare vertex; see (8).

with $\Lambda^{\mu}_{\mathrm{NA}}$ the non-Abelian term (see Fig. 3), and the ellipsis denotes contributions not considered here. The non-Abelian correction has the form

$$\Lambda^{\mu}_{\mathrm{NA}}(l,k) = \frac{N_c}{2}\int_q \widetilde{\Gamma}_\alpha(l_1,-q_1)\,S(q_3)\widetilde{\Gamma}_\beta(l_2,-q_2) \times \Gamma^{\alpha'\beta'\mu}_{3g}(q_1,q_2,p_3)D^{\alpha\alpha'}(q_1)D^{\beta\beta'}(q_2)\,, \tag{8}$$

where the internal vertices $\widetilde{\Gamma}^{\mu}$ retain only the tree-level tensor structure and are supplemented by an enhancement factor in the infrared. Such an enhancement is needed in order to account for the effect on the quark–gluon vertex of higher loop terms in the 2PI effective action. An alternative to this is using a 3PI or higher effective action to define the truncation, which means that both vertices and propagators are fully dressed and independent objects [15,18]. Further details on (8) and its solution can be found in [12].

A second functional derivative of the effective action with respect to the quark propagator defines the quark–antiquark BSE interaction kernel $K^{q\bar{q}}$ [14–16,18,19]. Equivalently,

$$\big[K^{q\bar{q}}\big]_{ik;lj} = -\frac{\delta}{\delta\big[S(x,y)\big]_{kl}}\big[\Sigma\,(x',y')\big]_{ij}\,, \tag{9}$$

followed by a Fourier transform to momentum space. This is the kernel that appears in the BSE description of a meson as a quark–antiquark bound state

$$\big[\Gamma_M(p,P)\big]_{ij} = \int_k \big[K^{(q\bar{q})}\big]_{ik;lj}\big[\chi_M(k,P)\big]_{kl}\,, \tag{10}$$

where $\Gamma_M(p,P)$ is the Bethe–Salpeter amplitude and $\chi_M(k,P) = S(k_+)\Gamma_M(k,P)S(k_-)$ its wavefunction. The quantum numbers of the state are defined by its covariant decomposition [30–32]. This gives access to both the mass of the bound-state as well as details of its internal structure.

The crucial motivation for such a definition of the Bethe–Salpeter kernel is that chiral symmetry, as expressed via the axial-vector Ward–Takahashi identity (axWTI)

$$\big[\Sigma(p_+)\gamma_5 + \gamma_5\Sigma(p_-)\big]_{ij} = \int_k \big[K^{(q\bar{q})}\big]_{ik;lj}\big[S(k_+)\gamma_5 + \gamma_5 S(k_-)\big]_{kl}\,, \tag{11}$$

is correctly implemented in the calculation of meson properties [33]. This guarantees, in particular, the identification of the pion as a Goldstone boson in the chiral limit.

With the truncation of the vertex DSE given in (8), the cutting process gives rise to a quark–(anti)quark kernel, given in Fig. 4, whose topology is analogous to a gluon ladder

$$\big[K^{(q\bar{q})}\big]_{ij;mn} = D_{\mu\nu}(q)\Big[\big[\gamma^\mu\big]_{ij}\big[\gamma^\nu\big]_{mn} + \big[\gamma^\mu\big]_{ij}\big[\Lambda^\nu\big]_{mn} + \big[\Lambda^\mu\big]_{ij}\big[\gamma^\nu\big]_{mn}\Big]\,. \tag{12}$$

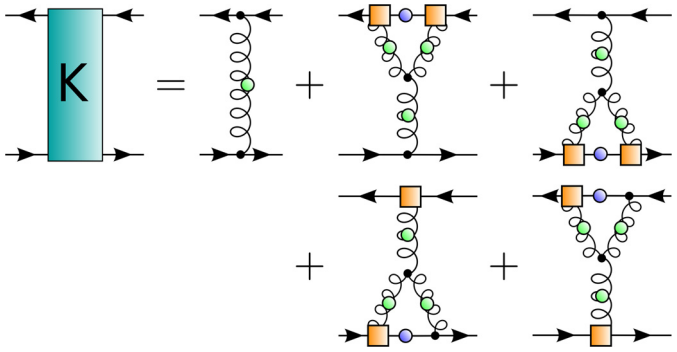

Fig. 4. The quark–antiquark kernel beyond rainbow-ladder.

This, taken with the truncated quark–gluon vertex above, satisfies chiral symmetry by construction. Further corrections to the quark–gluon vertex, in particular those featuring additional quark propagators, yield different topologies and/or are higher loop order; they are beyond the scope of the present work but can in principle be included.

It is important to stress that when the 2PI effective action is used to define the truncation at the level of vertex functions, the expansion must be chosen such that the functional derivative (9) can be formally performed to define the chiral-symmetry preserving BSE kernels. This implies that it must be possible to resolve diagrammatically the quark lines in the vertex corrections (7). This is the reason why quark–gluon vertices defined as ansätze are difficult to accommodate (and, hence, test) consistently in this framework.

It is illustrative to consider here the case of the two-loop expansion of the 2PI effective action, which leads to the well-known rainbow-ladder truncation. There, suppressing constants and color factors for simplicity, we have

$$\big[\Sigma(p)\big]_{ij} \simeq \int_k \big[\gamma^\mu S(q)\gamma^\nu\big]_{ij}D_{\mu\nu}(k)\,, \tag{13}$$

from which a functional derivative provides the kernel

$$\big[K^{(q\bar{q})}\big]_{ik;lj} \simeq \big[\gamma^\mu\big]_{ik}\big[\gamma^\nu\big]_{lj}D_{\mu\nu}(q)\,. \tag{14}$$

In practical calculations the gluon propagator is modelled by a phenomenological function which includes the aforementioned infrared enhancement of the quark–gluon vertex from (omitted) higher order corrections.

Since we wish to also consider bound-states of three-quarks, it proves useful as an intermediate step to formulate the diquark bound-state

$$\big[\Gamma_D(p,P)\big]_{ij} = \int_k \big[K^{(qq)}\big]_{ik;lj}\big[\chi_D(k,P)\big]_{kl}\,, \tag{15}$$

with diquark amplitude $\Gamma_D(p,P)$ and wavefunction $\chi_D(k,P) = S(k_+)\Gamma_D(k,P)S^T(-k_-)$. The superscript T denotes transposition; the covariant decomposition of a J^{-P} diquark Γ_D are that of a J^P meson $\Gamma_M C$ together with a charge conjugation matrix. The corresponding diquark kernel is then

$$\big[K^{(qq)}\big]_{ik;lj} = \big[K^{(q\bar{q})}\big]_{ik;jl}\,, \tag{16}$$

that is, it amounts to a transposition of the lower spin-line. For general ladder-like kernels, such as that in (14) the color factors are $(N_c^2-1)/2N_c$ and $-(N_c+1)/2N_c$ for a meson and diquark, respectively.

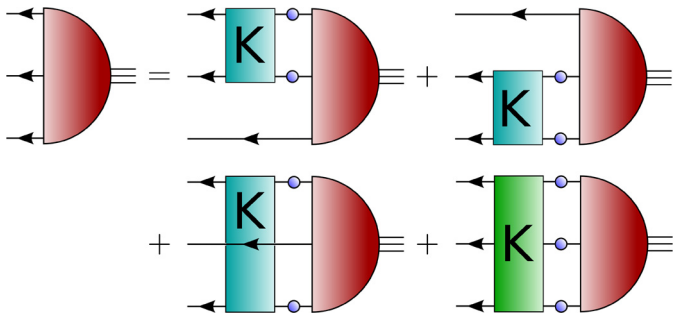

Fig. 5. The covariant Faddeev equation for the baryon, see (17).

Table 1
Meson masses and pion decay constant in GeV as calculated in rainbow-ladder [5] and beyond rainbow-ladder. Results affixed with † are fitted values.

	RL	BRL	PDG [35]
0^{-+} (π)	$0.14^{\dagger}$	$0.14^{\dagger}$	0.14
0^{++} (σ)	0.64	0.52	0.48(8)
1^{--} (ρ)	0.74	0.77	0.78
1^{++} (a_1)	0.97	0.96	1.23(4)
1^{+-} (b_1)	0.85	1.1	1.23
f_π	$0.092^{\dagger}$	0.103	0.092

The analogue of the Bethe–Salpeter equation for baryons can now be formulated. It contains the permuted sum of the two-body quark–quark kernel $K^{(qq)}$ and an irreducible three-body kernel $K^{(qqq)}$ [15,34]

$$\Psi = \left[K^{(qqq)}\right] G_0^{(3)} \Psi + \sum_{a=1}^{3} \left[K_a^{(qq)}\right] S_a^{-1}\, G_0^{(3)} \Psi\,, \tag{17}$$

see Fig. 5. We use here a compact notation, omitting indices, where implied discrete and continuous variables are summed or integrated over, respectively. Here $G_0^{(3)}$ represents the product of three fully-dressed quark propagators S. The subscript a labels the quark spectator to the two-body interaction. At the truncation level of the 2PI effective action we will consider in this work, the irreducible three-body force is identically zero [18]. The two-body kernel follows, as before, from the quark and quark–gluon vertex DSE.

3. Results

A consistency check that chiral symmetry is correctly implemented is provided by calculating the pion mass in the chiral limit. Finding a massless pion, as we indeed do, serves as a verification that the numerics are under control.

In [12] the internal vertices were adjusted to both resemble the tree-level component of the calculated vertex, and to yield a running quark mass in agreement with lattice calculations. Once the vertex truncation is defined, the only free parameter left is the current-quark mass. The light quark mass is then fixed to $m_{u/d} = 3.7$ MeV at the renormalization point 19 GeV so that the physical pion mass is obtained.

In Table 1 we show the ground-state meson masses below 1.4 GeV for two quark flavors for rainbow-ladder (using the Maris–Tandy interaction [5]) and for the beyond rainbow-ladder truncation presented here. The case of the scalar and vector states is remarkable in that their masses agree well with the experimental value of the ρ- and σ-mesons; this is, however, an unexpected feature. On the one hand, it is well known that unquenching effects (absent in this calculation) such as pion-cloud corrections [21,23,36] and effects associated with decay processes [37,38] provide extra attraction for vector and/or scalar channels. On the other hand, it is not yet settled whether the physical σ-meson originates (at least in part) form a $q\bar{q}$ state. Moreover, even if that was the case, the measured mass would be the result of the dynamical coupling of this *bare* state with several other channels [39,40]. In this respect, it is interesting to note that several DSE/BSE calculations [6,9,32], including the present one, generate a relatively light scalar $q\bar{q}$ state and hence suggest that the picture of a purely dynamical origin of the σ-resonance is not realized; this can likely be traced to the back-coupling of the quark–gluon vertex to the vertex itself and will be remedied at higher order in loops or in nPI.

Table 2
Baryon masses in GeV as calculated in rainbow-ladder [34,41–43] and beyond rainbow-ladder.

	RL	BRL	PDG [35]
$1/2^+$ (N)	0.94	1.05	0.94
$1/2^-$ (N^*)	1.16	1.08	1.54(1)
$3/2^+$ (Δ)	1.22	1.24	1.23

The previous remarks can be summarized in that one would expect our *quark-core* calculation to lead, in general, to heavier meson masses. The fact that this is not the case is an indication that other mechanisms, absent in the present calculation, are of relevance even in the ground-state meson sector. Additional support for this is found in the $a_1/b_1 - \rho$ and $a_1 - b_1$ splitting; whereas the former is improved with respect to the RL value, the latter is exceedingly large showing an imbalance in the different components of the present quark–gluon vertex.

Let us now turn our attention to baryons. In Table 2 we show the calculated nucleon and delta-baryon masses. We also calculated the mass of the nucleon parity partner $1/2^-$, as it is the first signature of the failure of RL in the baryon sector. Clearly, the masses for positive-parity states are slightly overestimated. This suggests that the simple quark-core picture supplemented with pion-cloud effects [20,23,24,36,44] could be realized for ground-state baryons. The possibility that ground-state baryons are, in contrast to mesons, less sensitive to the details of the quark–gluon interaction is an interesting one. It explains why the simple rainbow-ladder truncation has been thus far so successful in describing baryon properties [34,41–43].

The situation for excited baryons does not appear to be so simple. In RL the negative-parity nucleon comes out extremely light [42] unless one inflates the interaction strength [45,46], thus spoiling the agreement for other observables. The present calculation, using a genuine (albeit truncated) solution of a QCD-vertex DSE, does not improve on the situation of the nucleon's negative-parity partner. This result by itself already makes a case for the systematic introduction of interaction mechanisms, as it is not known *a priori* whether missing Abelian and/or non-Abelian mechanisms are leading in determining the spectrum of (bare) baryon resonances.

Another interesting aspect of using as interaction a solution of the quark–gluon vertex DSE is that it naturally features a quark-mass dependence of the interaction strength. One class of observables in which such a mass dependence is manifest are the baryon sigma terms. Calculated here using the Feynman–Hellmann theorem, they measure the dependence of the baryon mass on the quark mass. As shown in Table 3, these are exceedingly small in RL, owing to the quark-mass independence of the effective interaction. This changes dramatically in the present calculation. For the nucleon we now obtain a value in reasonable agreement with the upper limit of the consensual range [47–51]. For the delta, although there is no well-established value to serve as a reference, we find a similarly large result for the sigma term. However, this

Table 3
Sigma terms in MeV as calculated in rainbow-ladder and beyond rainbow-ladder.

	RL	BRL	Other [47–55]
$1/2^+$ (N)	30	60	25–60
$3/2^+$ (Δ)	24	63	32–79

could be related to the absence of decay mechanisms that induce non-analytic behaviors in the baryon-mass curve near the physical point.

4. Summary

In summary, we presented the first calculation of both mesons and baryons in a mutually consistent truncation of the quark–gluon vertex beyond rainbow-ladder. Being fixed in accordance to the 2PI effective action at three-loops, the freedom to adjust model parameters is limited and hence the bulk features of the results for the meson and baryon masses cannot presently be altered. Extensions must therefore be made that either take into account higher loop corrections to the effective action, or as we envisage, to incorporate vertices dynamically into the expansion by considering 3PI actions and beyond [18].

Regardless, the means to connect quarks and gluons presented here via symmetry preserving and calculated interaction vertices is both an important technical and conceptual achievement that, being in itself independent of the particular ansatz, can be systematically applied to *e.g.* crossed ladder and other higher order corrections to the kernel. Being intrinsically dependent upon the quark flavor and hence the quark mass, it will form the basis of future investigations of the baryon octet-decuplet [43] and meson nonet for the strange quark [32,56], as well as heavy-quark studies of charmonium and bottomonium [57–59]. Furthermore, the impact of corrections beyond rainbow-ladder on the internal structure of the hadrons can be tested through the calculation of electromagnetic form-factors [60–62].

Acknowledgements

We thank Gernot Eichmann, Christian S. Fischer and Walter Heupel for discussions and a critical reading of this manuscript. This work has been supported by an Erwin Schrödinger fellowship J3392-N20 and a Lise-Meitner fellowship M1333-N16 from the Austrian Science Fund (FWF), by the Helmholtz International Center for FAIR within the LOEWE program of the State of Hesse, and by the DFG collaborative research center TR 16.

References

[1] A. Bashir, L. Chang, I.C. Cloët, B. El-Bennich, Y.X. Liu, C.D. Roberts, P.C. Tandy, Commun. Theor. Phys. 58 (2012) 79.
[2] G. Eichmann, J. Phys. Conf. Ser. 426 (2013) 012014.
[3] I.C. Cloët, C.D. Roberts, Prog. Part. Nucl. Phys. 77 (2014) 1.
[4] P. Maris, C.D. Roberts, Phys. Rev. C 56 (1997) 3369.
[5] P. Maris, P.C. Tandy, Phys. Rev. C 60 (1999) 055214.
[6] L. Chang, C.D. Roberts, Phys. Rev. Lett. 103 (2009) 081601.
[7] L. Chang, Y.X. Liu, C.D. Roberts, Phys. Rev. Lett. 106 (2011) 072001.
[8] L. Chang, C.D. Roberts, Phys. Rev. C 85 (2012) 052201.
[9] W. Heupel, T. Goecke, C.S. Fischer, Eur. Phys. J. A 50 (2014) 85.
[10] P. Watson, W. Cassing, P.C. Tandy, Few-Body Syst. 35 (2004) 129.
[11] C.S. Fischer, R. Williams, Phys. Rev. Lett. 103 (2009) 122001.
[12] R. Williams, Eur. Phys. J. A 51 (5) (2015) 57.
[13] J. Berges, Phys. Rev. D 70 (2004) 105010.
[14] R. Fukuda, Prog. Theor. Phys. 78 (1987) 1487.
[15] M. Komachiya, M. Ukita, R. Fukuda, Phys. Rev. D 40 (1989) 2654.
[16] D.W. McKay, H.J. Munczek, Phys. Rev. D 40 (1989) 4151.
[17] M.E. Carrington, Y. Guo, Phys. Rev. D 83 (2011) 016006, arXiv:1010.2978 [hep-ph].
[18] H. Sanchis-Alepuz, R. Williams, arXiv:1503.05896 [hep-ph].
[19] J.M. Cornwall, R. Jackiw, E. Tomboulis, Phys. Rev. D 10 (1974) 2428.
[20] M.B. Hecht, M. Oettel, C.D. Roberts, S.M. Schmidt, P.C. Tandy, A.W. Thomas, Phys. Rev. C 65 (2002) 055204.
[21] C.S. Fischer, D. Nickel, J. Wambach, Phys. Rev. D 76 (2007) 094009.
[22] C.S. Fischer, D. Nickel, R. Williams, Eur. Phys. J. C 60 (2009) 47.
[23] C.S. Fischer, R. Williams, Phys. Rev. D 78 (2008) 074006.
[24] H. Sanchis-Alepuz, C.S. Fischer, S. Kubrak, Phys. Lett. B 733 (2014) 151.
[25] J. Braun, L. Fister, J.M. Pawlowski, F. Rennecke, arXiv:1412.1045 [hep-ph].
[26] R. Williams, EPJ Web Conf. 3 (2010) 03005.
[27] M. Hopfer, A. Windisch, R. Alkofer, PoS (2012) 073.
[28] A.C. Aguilar, D. Binosi, D. Ibáñez, J. Papavassiliou, Phys. Rev. D 90 (6) (2014) 065027.
[29] M. Mitter, J.M. Pawlowski, N. Strodthoff, Phys. Rev. D 91 (2015) 054035, arXiv:1411.7978 [hep-ph].
[30] C.H. Llewellyn-Smith, Ann. Phys. 53 (1969) 521.
[31] A. Krassnigg, M. Blank, Phys. Rev. D 83 (2011) 096006.
[32] C.S. Fischer, S. Kubrak, R. Williams, Eur. Phys. J. A 50 (2014) 126.
[33] H.J. Munczek, Phys. Rev. D 52 (1995) 4736.
[34] G. Eichmann, R. Alkofer, A. Krassnigg, D. Nicmorus, Phys. Rev. Lett. 104 (2010) 201601.
[35] K.A. Olive, et al., Particle Data Group, Chin. Phys. C 38 (2014) 090001.
[36] M. Oertel, M. Buballa, J. Wambach, Phys. At. Nucl. 64 (2001) 698, Yad. Fiz. 64 (2001) 757.
[37] D.B. Leinweber, A.W. Thomas, K. Tsushima, S.V. Wright, Phys. Rev. D 64 (2001) 094502.
[38] C.R. Allton, W. Armour, D.B. Leinweber, A.W. Thomas, R.D. Young, Phys. Lett. B 628 (2005) 125.
[39] J.R. Peláez, Phys. Rev. Lett. 92 (2004) 102001.
[40] M. Döring, C. Hanhart, F. Huang, S. Krewald, U.-G. Meissner, Phys. Lett. B 681 (2009) 26.
[41] H. Sanchis-Alepuz, G. Eichmann, S. Villalba-Chávez, R. Alkofer, Phys. Rev. D 84 (2011) 096003.
[42] H. Sanchis-Alepuz, S. Kubrak, C. Fischer, Int. J. Mod. Phys. Conf. Ser. 26 (2014) 1460121.
[43] H. Sanchis-Alepuz, C.S. Fischer, Phys. Rev. D 90 (9) (2014) 096001.
[44] G. Eichmann, R. Alkofer, I.C. Cloët, A. Krassnigg, C.D. Roberts, Phys. Rev. C 77 (2008) 042202.
[45] D.J. Wilson, I.C. Cloët, L. Chang, C.D. Roberts, Phys. Rev. C 85 (2012) 025205.
[46] J. Segovia, B. El-Bennich, E. Rojas, I.C. Cloët, C.D. Roberts, S.S. Xu, H.S. Zong, arXiv:1504.04386 [nucl-th].
[47] R.D. Young, A.W. Thomas, Phys. Rev. D 81 (2010) 014503.
[48] R. Horsley, et al., QCDSF-UKQCD Collaboration, Phys. Rev. D 85 (2012) 034506.
[49] S. Durr, Z. Fodor, T. Hemmert, C. Hoelbling, J. Frison, S.D. Katz, S. Krieg, T. Kurth, et al., Phys. Rev. D 85 (2012) 014509.
[50] P.E. Shanahan, A.W. Thomas, R.D. Young, Phys. Rev. D 87 (7) (2013) 074503.
[51] G.S. Bali, et al., Nucl. Phys. B 866 (2013) 1.
[52] V.E. Lyubovitskij, T. Gutsche, A. Faessler, E.G. Drukarev, Phys. Rev. D 63 (2001) 054026.
[53] I.P. Cavalcante, M.R. Robilotta, J. Sa Borges, D. de, O. Santos, G.R.S. Zarnauskas, Phys. Rev. C 72 (2005) 065207.
[54] G. Erkol, M. Oka, Phys. Lett. B 659 (2008) 176.
[55] V.V. Flambaum, A. Holl, P. Jaikumar, C.D. Roberts, S.V. Wright, Few-Body Syst. 38 (2006) 31.
[56] S.x. Qin, L. Chang, Y.x. Liu, C.D. Roberts, D.J. Wilson, Phys. Rev. C 85 (2012) 035202.
[57] E. Rojas, B. El-Bennich, J.P.B.C. de Melo, Phys. Rev. D 90 (2014) 074025.
[58] T. Hilger, C. Popovici, M. Gómez-Rocha, A. Krassnigg, Phys. Rev. D 91 (3) (2015) 034013.
[59] C.S. Fischer, S. Kubrak, R. Williams, Eur. Phys. J. A 51 (2015) 10.
[60] P. Maris, P.C. Tandy, Phys. Rev. C 65 (2002) 045211.
[61] G. Eichmann, Phys. Rev. D 84 (2011) 014014.
[62] G. Eichmann, C.S. Fischer, Eur. Phys. J. A 48 (2012) 9.